# Simulation of a High-convergence Electron Optics System for an X-band High-impedance Relativistic Klystron

**Danni Zhu**, **Jun Zhang**, **Zumin Qi**, **and Wei Li**
College of Optoelectric Science and Engineering
National University of Defense Technology, Changsha 410073, China

**Abstract**— The high-impedance relativistic klystron based on the hot cathode, of high power, long pulse, high efficiency and stable amplitude and phase, is one of the promising candidates for the high-power microwave coherent power combing. As a high-quality, small radius electron beam plays a crucial role in an effective beam-wave interaction, a high-convergence electron optics system is required for an 11.424 GHz high-impedance relativistic klystron, with an output power of 105 MW. In the design, to alleviate the cathode loading due to high-convergence, the uniformity of the cathode emittance and the laminarity of beam are both sacrificed. Then serious space charge effect is likely to occur with a rather high current density. To minimize the scalloping, it is difficult to provide the best overlap of the beam trajectories and magnetic force lines with priority to the amplitude of magnetic flux at the cathode. With the synthesis of Pierce's electron gun and the cylindrical focusing electrode, a particle in cell model of the electron gun is constructed to obtain the electrostatic characteristics of the electron beam. Based on the electrostatic beam trajectories, a beam-focusing system is designed, with which electron beam can be well focused by adjusting the magnetic field profile especially in the transient region. The PIC simulation results indicate that the balance radius of the reasonably fluctuated beam is about 3 mm ,with a fine laminarity, and the transmission, the perveance and the area convergence are 100%, 0.9 μP and 97 : 1 respectively, which satisfy the requirement of the 11.424 GHz high-impedance relativistic klystron. Moreover, with the comparison between thermionic emission and explosive emission in PIC code, the micro-characteristics of beam shows the latter is tend to be more reliable.

## 1. INTRODUCTION

The 11.424 GHz klystron is under development as an alternative RF source for a next electron-positron linear collider by SLAC, KEK and BINP, with the highest output power of 75 MW [1, 2]. Moreover, the high-impedance relativistic klystron based on the hot cathode, owing to its high power, long pulse, high efficiency and stable amplitude and phase, becomes one of the promising candidates for the high-power microwave (HPM) coherent power combing. An effective beam-wave interaction in a high power X-band klystron requires a high-quality electron beam with small radius so that the electron optics system plays a crucial role in the performance of the device [3]. Although the 11.424 GHz klystron has been fabricated in SLAC, KEK and BINP, but discussions on simulation of a high-convergence electron optics system are scanty. However, in terms of time and funds, the simulation is an efficient way to ensure a satisfying performance of the beam-stick test in advance. Besides, there are several issues deserving deliberate consideration. Firstly, to alleviate the cathode loading due to high-convergence, the uniformity of the cathode emittance and the laminarity of beam are both sacrificed. Secondly, serious space charge effect is likely to occur with a rather high current density. Thirdly, to minimize the scalloping, it is difficult to provide the best overlap of the beam trajectories and magnetic force lines with priority to the amplitude of magnetic flux at the cathode.

This paper presents the design of a high-convergence electron optics system for an X-band high-impedance relativistic klystron by PIC simulation. In Section 2, the detailed design and optimization of electron gun are described and the electrostatic characteristics of beam is presented. In Section 3, a beam-focusing system well matched with the above beam is designed by a high-frequency structure simulator, and the typical particle-in-cell (PIC) simulation results indicate that the balance radius of the reasonably fluctuated beam is about 3 mm, and the beam voltage and current are 525 kV, 328 A respectively. Finally, a discussion on two cathode emission methods and a conclusion are given in Section 4.

## 2. ELECTRON GUN ELECTROSTATIC DESIGN

As the optimized parameters of the beam-wave interaction system are summarized in Table 1, the 11.424 GHz high-impedance relativistic klystron with power of 105 MW is already achieved in

PIC simulation [4]. It shows the target performance of the electron optics system that the beam voltage and current are 525 kV and 458 A respectively. Thus, the initial velocity due to the thermal emittance can be ignored under a high voltage. Fig. 1 indicates the best balance radius should be compressed to 3 mm. The average cathode loading over cathode is 13.5 A/cm$^2$ according to XB72K in KEK [5], implying the convergence of the cathode is as high as 117.

Table 1: Simulation parameters of the beam-wave interaction system.

| Beam voltage | Beam current | Beam radius (mean) | Drift tube radius | Perveance | Output Power | Gain | Efficiency |
|---|---|---|---|---|---|---|---|
| 525 kV | 458 A | 3.0 mm | 4.6 mm | 1.2 μP | 105 MW | 50 dB | 43.5 % |

The initial geometrical parameters are obtained from the synthesis method of the Pierce gun developed by Vaughan [6]. Since it doesn't take the anode hole aberrations into account, a cylindrical focusing electrode [7] is used to compensate as illustrated in Fig. 2. Furthermore, the synthesis method of the Pierce gun usually applying to convergence below 40 provides a rather rough geometric layout, which means special emphasis should be taken on the optimum gun geometry.

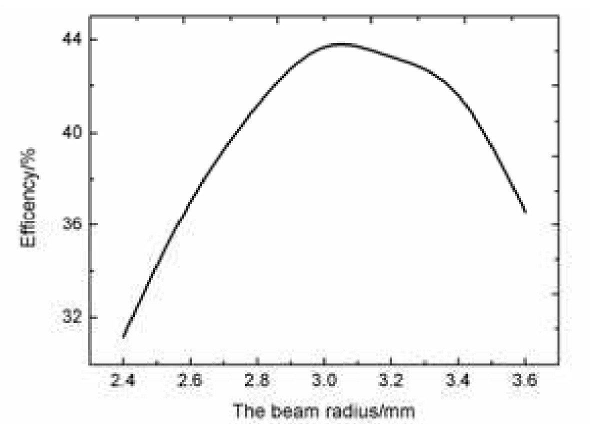


Figure 1: Extraction efficiency versus beam radius.

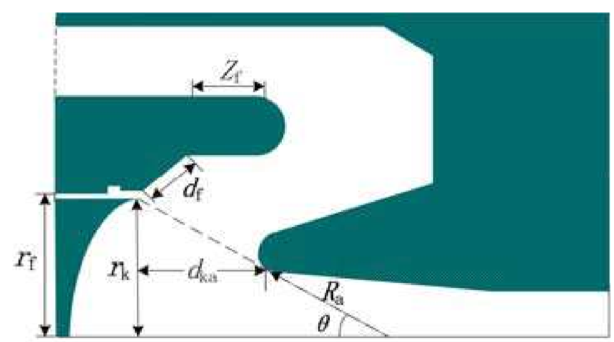


Figure 2: Electron gun model with cylindrical focusing electrode.

In order to realize a desirable high-convergence electron gun, the optimization routine is scheduled. Firstly, a suitable electric field contour distribution should be ensured as the beam trajectories always follow the magnetic force lines. Secondly, beam should be converged at least making the radius smaller than that of drift tube initially to avoid beam interception, and then by monitoring the beam current on different axial position the transmission of 100% through a drift tube is verified later. Thirdly, the target perveance and the beam radius are well worth considering, while the laminarity being kept as good as possible. Table 2 shows the main optimum gun geometric parameters.

Table 2: Main parameters of the electron gun.

| $r_k$/mm | $r_f$/mm | $Z_f$/mm | $d_f$/mm | $\theta$/° | $R_a$/mm | $d_{ka}$/mm |
|---|---|---|---|---|---|---|
| 31 | 33 | 10 | 20 | 28 | 28.5 | 48 |

In the optimization, it finds that the beam radius is mainly influenced by the geometric layout and position of the cylindrical focusing electrode, the perveance is sensitive to the position of anode so that it is adjusted by changing the gap between the cathode and the anode, and the laminarity of beam can be improved by decreasing the radius of cathode in small scale. According to Fig. 3(a), the length of focus electron should be long enough to strengthen the shielding for the cathode and depress the cathode edge loading, and the electrostatic force increases at the same time. Therefore, the beam trajectories are converged with the beam radius decreasing so that the space charge effect is enhanced with the beam current reducing gradually. On the other hand, the position of inner top section of the focusing electrode also plays a key role on the beam radius. As $d_f$ is increased, it results in both raising and extending the focusing electrode. In Fig. 3(b), when $d_f$ is below 20 mm the extension prevails so that the shielding is enhanced and hence the beam radius decreases. When $d_f$ is over 20 mm the raise prevails so that the shielding is weaken and hence the beam radius increases, and the space charge effect is weaken leading to the beam current rising.

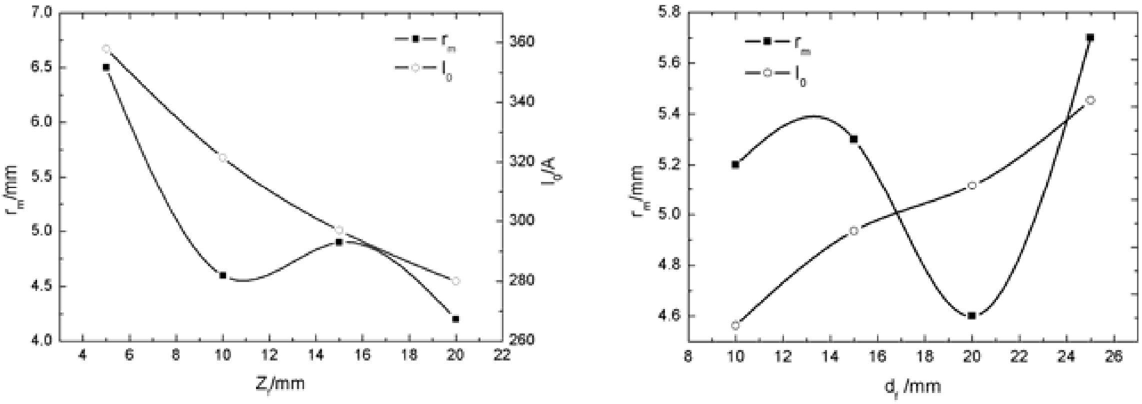


(a) (b)

Figure 3: Beam radius $r_m$ and the beam current $I_0$ versus the different structure. (a) Length $Z_f$ of focus electron. (b) Position $d_f$ of inner top section of the focusing electrode.

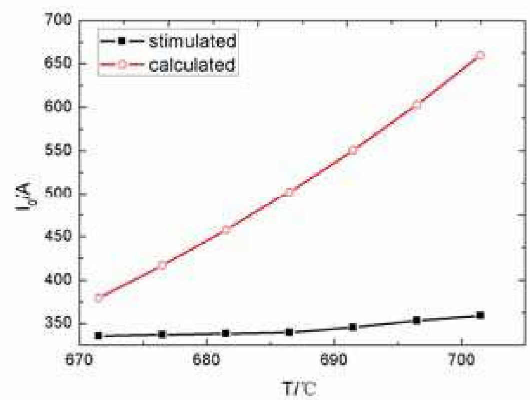


Figure 4: Beam current as a function of temperature in PIC simulation and theory.

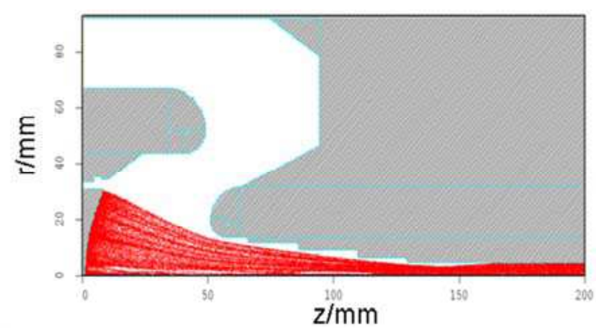


Figure 5: Final beam trajectories without magnetic field.

Under a high operating voltage, the voltage gradient in the electron gun becomes a critical issue. And the maximum gradient occurs at the top of the focusing electrode or the anode. In order to decrease the high-voltage gradient to a reliable level and confine the dimension of the gun, only the radius of the outer top section of the focusing electrode and anode are augmented to 15 mm and 12 mm respectively [8]. Further calculation indicates that the maximum gradient decreased to 360 kV/cm. For low operating temperature, the electron gun is a typical Pierce type with an oxide cathode. Based on Richardson-Dushman equation [9]

$$j_e = AT^2 e^{-\frac{e\phi}{KT}} \ \left(\mathrm{A/cm^2}\right) \tag{1}$$

where $k$ is the Boltzmann constant, $A_0$ is the Dushman parameter, and $\phi$ is the work function according to the material. In Fig. 4, as a function of temperature in both PIC simulation and Richardson-Dushman equation, the beam current is growing with the temperature rising whereas the growing rate is much smaller in simulation than that in theory. Therefore we can come into a conclusion that increasing the temperature does improve the cathode emittance ability in theory but the actual beam current is usually seriously limited by the space charge effect. Unfortunately, Richardson-Dushman equation is without taking this limitation into account.

The PIC simulation results of the gun without magnetic focusing are illustrated in Table 3, indicating the beam radius is compressed to 3.3 mm and the beam current is 328 A. The final beam trajectories are presented in Fig. 5, showing the beam transmission nearly of 100% and good laminarity. It can be seen that the beam-focusing system is indispensable to confine the scattered electrons intercepted by the tube through the drift region when the electrostatic focusing force vanished.

Table 3: Simulation results in electrostatic beam.

| $r_m$/mm | $I$/A | $j_k/(\text{A}\cdot\text{cm}^{-2})$ | $P$/μP | $M^2$ | $Z_m$/mm | $E/(\text{kV}\cdot\text{cm}^{-1})$ |
|---|---|---|---|---|---|---|
| 3.3 | 328 | 10.9 | 0.9 | 88:1 | 85 | 360 |

## 3. MAGNETIC CIRCUIT AND BEAM OPTICS

The beam-focusing system is a space-charge balanced flow type with a solenoidal field. The correlative magnetic flux densities are illustrated in Eq. (2) ∼ Eq. (4), including the Brillouin value $B_b$, one at the beam drift region $B_0$, and one at the cathode $B_k$, where $I$ and $U$ are current beam and voltage respectively, $r_0$ is the beam balance radius and $K$ is the shielding factor [10].

$$B_b = \frac{830}{r_0}\frac{I_0^{1/2}}{V_0^{1/4}}(Gs) \tag{2}$$

$$B_0 = B_b \Big/ \sqrt{1-K^2} \tag{3}$$

$$B_k = KB_0\left(\frac{r_0}{r_k}\right)^2 \tag{4}$$

Substitute $V_0 = 525\,\text{kV}$, $I_0 = 328\,\text{A}$, $r_0 = 3\,\text{mm}$ into the above equations when $K$ is set to be 0.9, then $B_0 = 4270\,\text{Gs}$, $B_k = 36\,\text{Gs}$ are obtained. This indicates the magnetic flux density at the beam drift region is 2.3 times as large as the Brillouin value. The geometric layout of the solenoidal magnet structure is presented in Fig. 6, containing six magnet coils and a solenoid yoke. On the outside of the front wall of the solenoid yoke, a trim coil marked coil1is set to tune the magnetic field near the cathode.

The arrangement for beam matching with the beam-focusing system is crucial to obtain perfect focusing beam characteristics, especially for the magnetic flux densities at the cathode and the entrance of the drift tube named transition region. The following basic guidelines to optimize the distribution of the magnetic flux are laid. On the one hand, the magnetic flux density at the cathode and one at the beam drift region should be approximate to $B_k$ and $B_0$. On the other hand, the best overlap of the initial beam trajectories and magnetic force lines specially in gun and anode hole regions should be achieved [6].

In the optimization process we also find several disciplines described below.

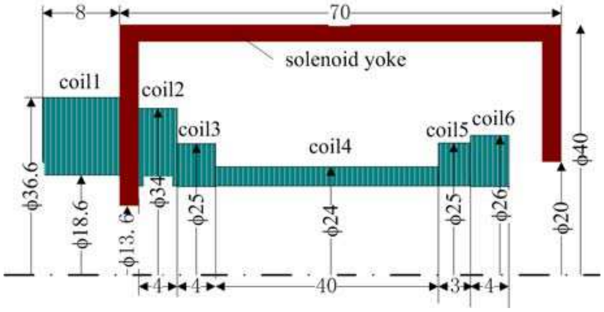


Figure 6: Diagram of the beam-focusing system (whose units are centimeters).

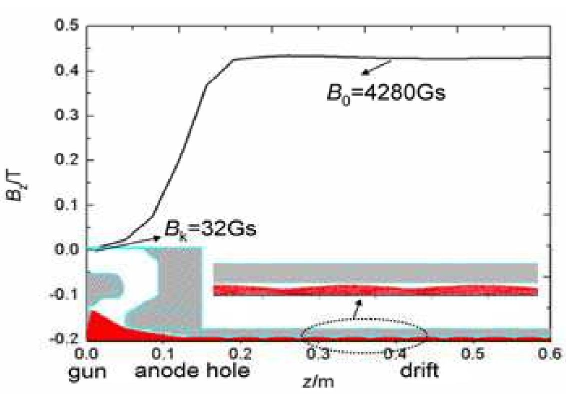


Figure 7: Magnetic profile and beam trajectories in the beam-focusing system.

1) Because the beam trajectories in whole region are sensitive to the magnetic flux density at the cathode, make priority to comply with the first principle.
2) Once the magnetic flux density at the cathode is too large, the beam is likely to be intercepted by the anode. Moreover, the low magnetic flux density just behind the anode hole in the transition region leads to the beam intercepted by the inner section of the anode.
3) In front of the drift tube of the transition region, the magnetic flux density should be $0.8B_0 \sim 0.9B_0$ to ensure the beam transmission 100% in this section.
4) After the perfect beam transmission is achieved, the stronger $B_k$ is, the larger the balance radius of beam is with lower beam ripple.
5) It is shown that the magnetic flux density behind the entrance of the drift region should be increased to $B_0$ in the transition region as soon as possible, or the laminarity of beam goes poor.

The magnetic flux density in the transition region is dependent on the aperture of the solenoid yoke and the main magnet coils. Through enlarging the aperture of the front-wall in the solenoid yoke, the magnetic flux density behind the anode hole in the transition region can be improved. And the magnetic flux density in the whole transition region can be enhanced by a large aperture of the back-wall. Notably, the decrease of magnetic field at the end of solenoid is essential to collect the scattered beam for high efficiency.

The relative location of the beam-focusing system respect to the electron gun also influences the beam balance radius, transmission, fluctuation and laminarity, which also needs to be optimized. If remove the beam-focusing system back 45 mm, the magnetic field profile just satisfies the above disciplines as shown in Fig. 7, which indicates that the magnetic field at the cathode is 32 Gs, and the longitudinal magnetic field in the interaction region is about 4280 Gs. With magnetic field profile introduced, the beam trajectories were carried out with the PIC code in Fig. 7, showing the beam transmission is about 100% with good laminarity and low ripple. The beam trajectories in drift region in detail shows the balance radius has reached 3.15 mm and hence the convergence is improved to 97 thanks to the secondary compression from the magnetic field.

Although the perveance is still 0.9 μP as the result without magnetic focusing, the simulation result of the beam-wave interaction system based on the final beam parameters with the obtained beam-focusing system shows the output power reaches 79 MW, with efficiency of 44.5% and gain of 49 dB.

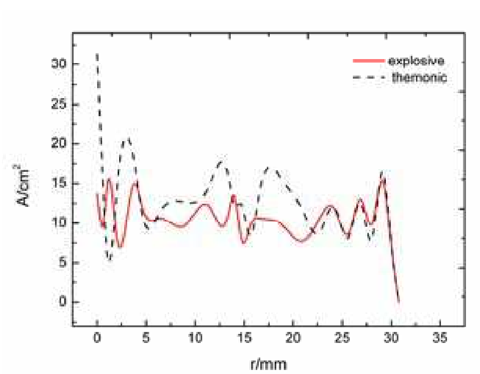


(a) current density distribution

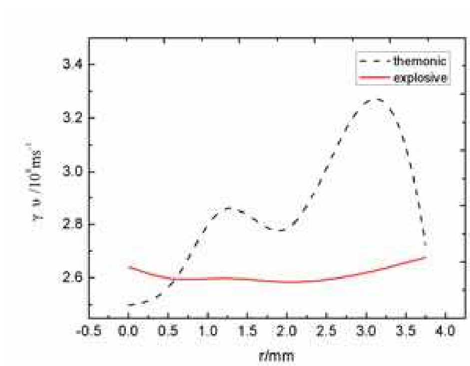


(b) electrons velocity distribution

Figure 8: Micro-characteristics of the beam distribution along the cathode radius.

## 4. DISCUSSION AND CONCLUSION

The above simulation is based on thermionic emission in PIC code, however the actual cathode emittance can also be simulated by explosive emission. Comparing the simulation results of these two cathode emission methods, the characteristics of beam are almost the same apart from the micro-characteristics as illustrated in Fig. 8. The current density distribution along the cathode radius is shown in Fig. 8(a). With a high-convergence, the cathode loading should not only be limited to a reasonable level but also have good uniformity. Therefore the simulation result by explosive emission is overwhelm the other one on the two points, whose average cathode loading is about $10\,\text{A/cm}^2$, lower than that by thermionic emission. Distribution of the electrons velocity across the beam are presented in Fig. 8(b), which is more homogeneous by explosive emission.

To summarize, the design of a high-convergence electron optics system for an X-band high-impedance relativistic klystron by PIC simulation is presented in this paper. The static electricity characteristic of the gun is optimized by the big curvature radius focusing electrode and anode to reduce the electric field. A match magnetic focus system is designed, with which the electron beam can be well focused. A solid beam is obtained with a radius of 3 mm, and the beam voltage and current are 525 kV and 328 A. The fluctuation on the beam is small with favorable laminar flow characteristic, and the transmission, the perveance and the area compression are 100%, 0.9 μP and 97, respectively. With the comparison between thermionic emission and explosive emission in PIC code, the micro-characteristic of beams shows the latter is tend to be more reliable.

## ACKNOWLEDGMENT

The authors would like to express their gratitude to the reviewer of this paper for his valuable comments and suggestions. The authors wish to express gratitude to Dr. X. J. Ge for his help in revising the English writing.

## REFERENCES

1. Matsumoto, S., S. Fukuda, and S. Kazakov, "Development of PPM-focused X-band pulse klystron," *Proceedings of the 2nd Annual Meeting of Particle Accelerator Society of Japan and the 30th Linear Accelerator Meeting*, 345–366, Tosu, Japan, Jul. 2005.
2. Sprehn, D., G. Caryotakis, and A. Haase, "Latest results in SLAC 75 MW PPM klystrons," *Proceedings of SPIE*, 85–90, Florida, America, Apr. 2000.
3. Wang, S., Y. Wang, J. Yang, et al., "The optics system for sheet beam of klystron with uniform magnetic focusing field," *Chinese Journal of Vacuum Science and Technology*, Vol. 27, 226, 2007.
4. Zhu, D., J. Zhang, W. Li, and Z. Qi, "Simulation study of an X-band high power relative klystron amplifier," *Laser Part. Beams*, Vol. 26, 505, 2014.
5. Chin, Y. H., K. Takata, S. Fukuda, H. Mizuno, S. Michizono, et al., "The 120 MW X-band klystron development at KEK," *Proc. of EPAC98*, 1894–1896, 1998.
6. Electronic Tube Design Handbook Editorial Committee, *The Optics System for Microwave Tube Design Handbook*, National Defense Industry Press, Beijing, 2010.
7. Zhao, G., W. Wang, and Y. Gong, "Design of the electron gun for S-band high power TWT," *Vacuum Electronics*, Vol. 5, 1921, 2006.
8. Zhang, R. and Y. Wang, "Design simulation of electron optics system for 100 megawatt klystron" *Chinese Journal of Vacumm Science and Technology*, Vol. 5, No. 29, 499–503, 2009.
9. Ding, Y., *Design, Manufacture and Application of High Power Klystron*, National Defense Industry Press, Beijing, 2010.
10. Feng, H., "The study of electron optics system for X-band klystron," 6, University of Electronic Science and Technology of China, Chendu, 2012.